$CuPbX_3$ and $AgPbX_3$ Inorganic Perovskites for Solar cell Applications

Taame Abraha Berhe[1#], Meng-Che Tsai[2#], Wei-Nien Su[1,*] and Bing-Joe Hwang[2,3,*]

[1]*NanoElectrochemistry Laboratory, Graduate Institute of Applied Science and Technology, National Taiwan University of Science and Technology, Taipei 106, Taiwan*
[2]*NanoElectrochemistry Laboratory, Department of Chemical Engineering, National Taiwan University of Science and Technology, Taipei 106, Taiwan*
[3]*National Synchrotron Radiation Research Center, Hsin-Chu, 30076, Taiwan*
Corresponding Authors: E-mail: bjh@mail.ntust.edu.tw (B.J. Hwang) and wsu@mail.ntust.edu.tw (W.N. Su)

Abstract

One of the possible solutions to the world's rapidly increasing energy demand is the development of new Photovoltaic device and photoelectrochemical cells with improved light absorption. This requires development of new semiconductor materials which have appropriate bandgap to absorb a large part of the solar spectrum at the same time as being stable in both the ambient and aqueous environments. Here, to the best of our knowledge, we showed computational identification of relevant fully inorganic ternary perovskites materials based on electronic structure calculations for the first time. Our first principles calculations were based on DFT as implemented in the VASP program. The identification is based on an efficient and reliable way of calculating semiconductor band gaps. We found that these materials are suitable for solar cell purpose since their optical bandgap ranged from 1.54 – 2.33 eV-computational calculation and 1.42 -1.93 eV-experimentally determined, which is similar to the $CH_3NH_3PbI_3$ hybrid perovskites. The outcome of the identification includes new ABX_3 type materials: $CuPbI_3$, $CuPbBr_3$, $CuPbCl_3$ and $AgPbX_3$, which warrant further experimental investigations. These materials are direct bandgap materials, which are suggested to absorb broad solar spectrum with distinct advantages in terms of its environmental stability.

Keywords New perovskites**,** $CuPbX_3$, $AgPbX_3$, bandgap, computational, development, identification

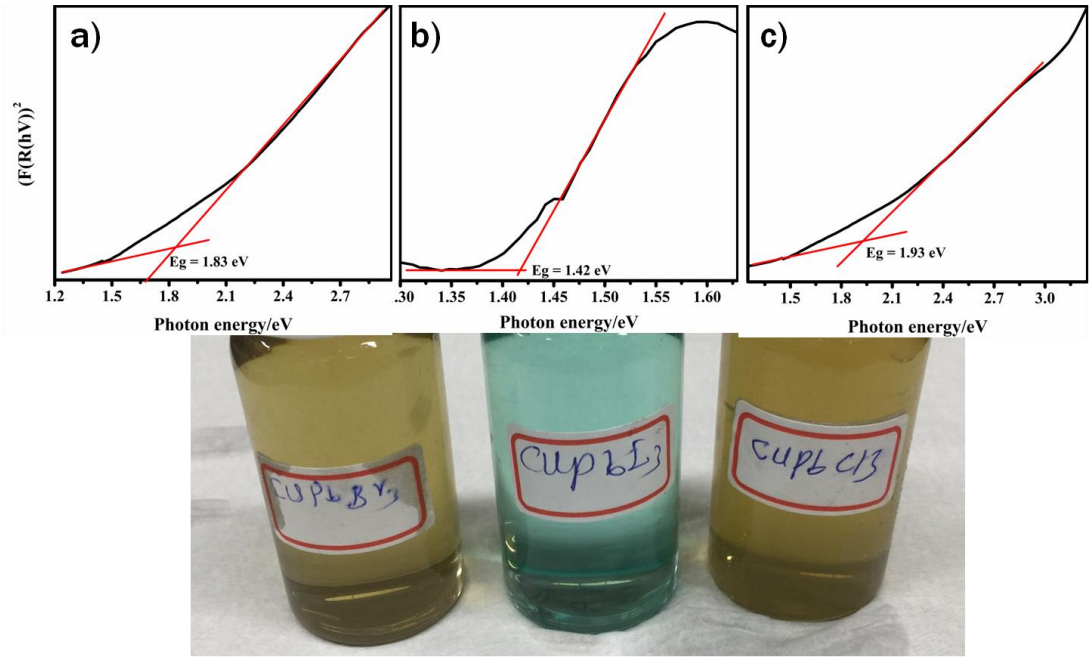

Introduction

Currently, the area of photovoltaics become revolutionized by newly emerging solar cells, organometal halide hybrid perovskites solar cell with its most recent efficiency jumps from 23%[1] into 29.15%.[2] Remarkably, $CH_3NH_3PbI_3$-based perovskites have very long electron and hole carrier diffusion lengths, high optical absorption, unique defect properties.[3-4] Furthermore, recent theoretical and experimental results have shown that $CH_3NH_3PbI_3$ exhibits ambipolar self-doping properties: both good p-type and n-type conductivities can be realized by manipulating the growth conditions.[5] Beside the exceptional high efficiency and V_{OC}, lead halide perovskites are also capable of bandgap tuning from about 1.5 eV ($CH_3NH_3PbI_3$) to 2.2 eV ($CH_3NH_3PbBr_3$) by changing the compositions of perovskites.[6] This capability makes lead halide perovskites as ideal candidates for all perovskites thin-film tandem cell and other optoelectronic device applications.

However, until now, it has been known that for all their gains in efficiency, organometal halide hybrid perovskites have faced stability challenges[7] due to presence of defects, disorder and heterogeneity on photoexcited carrier dynamics.[8] Mixed-cation perovskites solar cells have consistently outperformed their single-cation counterparts in both efficiency and stability cases. The first perovskites device to exceed 20% power conversion efficiency was fabricated with a mixture of methylammonium and formamidinium[9] and improved stability.[10-11] Recent reports have shown promising results with the introduction of cesium mixtures, enabling high efficiencies with improved photo-, moisture and thermal stability.[12] McGehee[12] reported exceptional stability for new perovskites recipes that replace an organic component called methylammonium with formamidinium or the element cesium. The combination of the more stable perovskite and the protection provided by the ITO layer allowed the cells to operate for more than 1000 hours in air and 40% humidity without significant degradation. When encapsulated to protect them from moisture, these cells showed no sign of degradation for six weeks, even when exposed to temperatures of 85°C and a relative humidity of 85% for 1000 hours, a standard test of durability. “Panels that pass it usually will not fail due to heat and humidity over 25 years outside,” McGehee says.[12,1] The increased moisture and thermal stability are especially important for various reasons including deposition of

metal oxide contacts through atomic layer deposition[13] or chemical vapour deposition that may require elevated temperatures or water as a counter reagent. With all these concerns, it is reasonable to find an alternative perovskites material that can improve the photo-, moisture and thermal stability issues of methylammonium based organolead halide hybrid perovskites solar cells. This is due to the reasons that methylammonium cation is weakly stable towards moisture and thermal treatments and it is more preferable to find materials[14-15] with reasonable stability and relatively high efficiency for practical applications.[7]

The materials community is currently witnessing a fundamental change in the way novel materials are designed and discovered. A steady increase in computational power, accompanied by developments in quantum theory and algorithmic breakthroughs that allow for efficient yet accurate quantum mechanical computations, opens the door to computing properties of a wide range of materials that once seemed prohibitively expensive. As a result, explorations of the vast chemical space are increasingly being pursued and have significantly aided our intuition and knowledge-base of material properties. In our previous work we synthesized bulk crystals of $MAPbI_3$.[16] We, herein, investigated crystal structure, electronic and optical properties of $CuPbI_3$, $CuPbBr_3$, $CuPbCl_3$ and $AgPbI_3$ fully inorganic new perovskites for the first time, with the purpose for more stable and optimal light absorption compared to the methylammonium based organometal halide perovskites. First Principles calculations were performed based on DFT calculation as implemented in the VASP program during which the spin-orbit effect was neglected. These materials are direct bandgap material, which allow direct band to band transition with theoretically calculated tunable bandgap ranged 1.54 eV-2.33 eV (theoretically calculated) and 1.42-1.93 eV(experimentally determined). This suggests that these materials are suitable for photovoltaic and other optoelectronic device applications such as laser, light emitting diode and photovoltaic devices, which require direct band to band transitions.

Result and discussion

Crystal structures/Geometric properties: Previous reports indicated that ABX_3 type compounds show various phases under different temperatures, but in the high temperature phase, all adopt a cubic perovskites structure[17], with a three-dimensional framework of corner-sharing BX_6 octahedron. Figure 1 shows the crystal structure for cubic $CuPbI_3$ perovskites. The primitive cell of this perovskites is consisting of corner-linked PbI_6 octahedral of the iodine atoms, with the Pb cation at their center and the Cu cation between them.[18] The structure of $CuPbI_3$ was relaxed first and the obtained lattice constant for this cubic material is 6.405Å after optimization with $\alpha = \gamma = \beta = 90.0°$ for the unit cell shown in Figure 1a. Volume of the cell is 6.405^3 Å^3. The bond lengths obtained from the relaxed structure are: Pb – I: 3.21, Pb – Pb: 6.42, Pb – Cu: 5.55, Cu – I: 4.53, Cu – Cu: 6.41, I – I: 4.53 Å as well as the effective coordination number is 6.00. The obtained space group was also determined to be Pm-3m. The calculated crystal structure parameters are presented in Table 1 Summary of crystal structure parameters

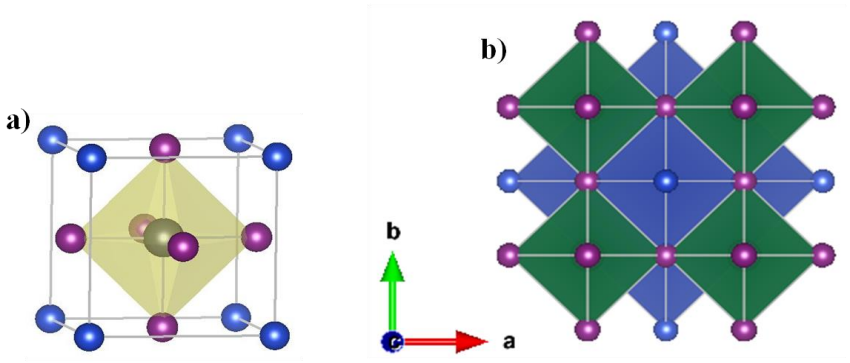

Figure 1 a) Unit cell and b) crystal structure for cubic $CuPbI_3$ perovskites, with blue color is Cu, purple is iodine and dark gray one is lead.

The tolerance factor is invented by Goldschmidt to describe the perovskites structure by taking three types of spheres in a perovskites-structure into account. Since the ionic radii are generally known, a tolerance factor can be calculated, that indicates the degree of compatibility of a given set of ions with the ideal, cubic perovskites structure. This relationship was first explored by Goldschmidt, in 1926[19], who suggested that it could be used to predict the likelihood that a pair of ions would form a perovskites structure phase.

The t value >1 implies the A cation is too large to fit in to their interstices and possible structures are hexagonal polytype; t = 0.9-1.0 indicates ideal condition with cubic perovskites; 0.71-0.9 –A cations are too small to fit in to their interstices with several possible structures such as orthorhombic and rhombohedral variants and t< 0.71 indicates A and B ions have similar ionic radii with possible close packed structures. For this purpose, it is assumed that for a stable structure to form the cations, just touch the surrounding anions (Goldschmidt's rule), then: $t = (r_A + r_X)/(r_B + r_X) = \sqrt{2}$ or, where t is called the tolerance factor, r_A is the radius of the cage site cation, r_B is the radius of the octahedrally coordinated cation and r_X is the radius of the anion. Goldschmidt's proposal was that a stable perovskites structure phase would form if the value of the tolerance factor, t, was close to 1.0. However, this is applicable at room temperature to the empirical ionic radii. The tolerance factor for $CuPbI_3$ at room temperature is 0.801 nm which could be tetragonal structure. The cubic unit cell edge, a, is equal to twice the B─X bond length: 2(B−X) = a. The width of the cuboctahedral cage site, √2a, is equal to twice the A─X bond length: 2(A-X) = √2a. This means that the ideal structure forms when the ratio of the bond lengths is given by: (A-X)/(B-X) = √2. .Because many perovskites structures have been described, it is now usual to use the measured bond lengths in the crystal rather than ionic radii to give an observed tolerance factor t_{obs}: t_{obs} = (A-X)/√2(B-X), where (A─X) is the average of the measured bond lengths between the A cation and the surrounding 12 anions and (B─X) is the average of the measured bond lengths between the B cation and the surrounding six anions. For $CuPbI_3$ perovskites, a is 2x3.2025 = 6.405Å, width of the cuboctahedral cage site is 2x4.53 equal to 9.06 Å and the tolerance factor given by the average bond length is 1.00 for all the perovskites materials. The stable structure is cubic structure for this material at high temperature. Error! Reference source not found. shows cubic crystal structures of $CuPbX_3$ derived by replacing $CH_3NH_3^+$ cation using Cu^+. The calculated X-ray diffraction pattern of $CuPbX_3$ (X = I, Br & Cl) is presented in **Figure 2** the diffraction patterns are observed shifting towards higher 2Theta values. This indicated that the volume compression due to the decrease of ionic radii from iodine to chlorine. Thus the volume of the unit cell depends on the Pb-X bond length and radius of the halogens. As shown from **Table 1** the volume of the cell is observed to decrease from 262.76 Å^3 to 181.94 Å^3. Similarly, the cubic crystal structure

and diffraction pattern for partial replacement of iodine are presented in **Figure S3** and

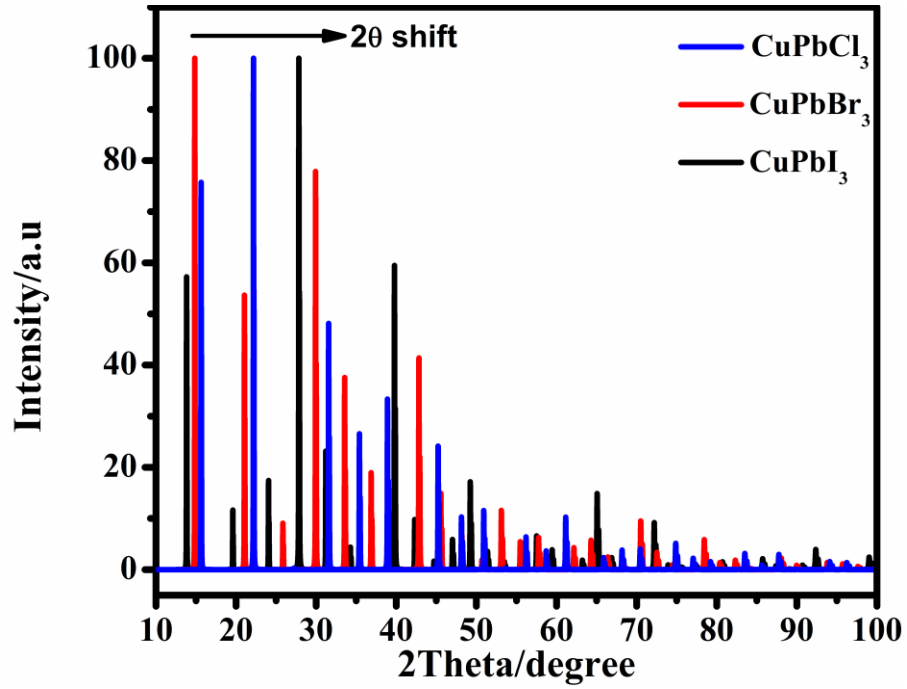

showed similar behavior.

Figure 2 Simulated X-ray diffraction pattern: a) $CuPbI_3$ (black line), b) $CuPbBr_3$ (red line) and $CuPbCl_3$ (blue line). The black arrow indicated the shift of diffraction pattern with variation in halogen atoms, verifying the volume compression from I to Cl containing $CuPbX_3$ perovskites due to shrink of Pb-Cl bond length compared to Pb-I bond length. We first relax the structures of all the cubic ABX_3 type compounds. The obtained lattice constants are shown in Table 1. We find that the lattice constants of ABX_3 increase with increasing the size of X from Cl, to Br and I.

Table 1 Summary of crystal structure parameters

Perovskites type	**Lattice parameter**		**Unit-cell volume**	**Space group**	**Bond length/ Å**	**t**	**Bandgap, Eg, eV**
$CuPbI_3$	a =b=c= 6.405	α=β=γ= 90.00	262.76 Å^3	Pm-3m	Pb-I = 3.20 Cu-I = 4.53 Pb-Cu =5.54	1	1.56[a]/1.42[b]
$CuPbBr_3$	a =b=c= 5.96	α=β=γ= 90.00	212.53 Å^3	Pm-3m	Pb-Br = 2.98 Cu-Br =4.21 Pb-Cu =5.17	1	1.88[a]/1.83[b]
$CuPbCl_3$	a =b=c= 5.66	α=β=γ= 90.00	181.94 Å^3	Pm-3m	Pb-Cl = 2.83 Cu-Cl =4.00 Pb-Cu =4.91	1	2.33[a]/1.93[b]
$AgPbI_3$	a =b=c= 6.4025	α=β=γ= 90.00	262.76 Å^3	Pm-3m	Pb-I = 3.20 Cu-I = 4.53	1	1.57

					Pb-Cu =5.54		
$AgPbBr_3$	a =b=c= 5.97	α=β=γ= 90.00	212.54 Å$^{\wedge 3}$	Pm-3m	Pb-Br = 2.99 Ag-Br =4.22 Pb-Cu =5.18	1	1.88
$AgPbCl_3$	a =b=c= 5.68	α=β=γ= 90.00	183.44 Å$^{\wedge 3}$	Pm-3m	Pb-Cl = 2.83 Ag-Cl =4.01 Pb-Ag =4.92	1	2.34

[a] and [b] theoretically and experimentally calculated bandgap, respectively.

Electronic and optical properties of $CuPbX_3$: Based on the relaxed structures, we first calculated the band gap of these materials, which is the key quantity for selecting solar-cell materials. Figure 3a presents the band structure and the partial density of states (PDOS) for cubic ABX_3 like structures of $CuPbX_3$. The valence band maximum (VBM) consists of the Pb 6s and X p orbitals, whereas conduction band minimum (CBM) is dominated by Pb 6p orbitals. Furthermore, these materials showed direct bandgap ranged from 1.56 -2.33 eV. The top of the valence band is located at the R symmetry point in the first Brillouin zone. The reported band gap value of hexagonal $CuPbI_3$ thin film deposited by solution based method and high vacuum method indicated 1.82[20] and 1.64 eV[21], respectively. This optical band gap value also agrees with the band gap value calculated for phase change in $CH_3NH_3PbI_3$ by UV–Vis spectroscopy.[22] It is also reported that the presence of methylammonium cation or Cs^+ does not affect the band gap region[23] and it is the inorganic component of lead halide perovskites that play a dominant role in ascertaining the band gap energy.[24-25] Similarly, it has been reported that replacement of $CH_3NH_3^+$ or Cs^+ by a univalent transition d^{10} metal ions, e.g., Cu^+ did not affect the band gap.[20] Naeem et.al. revealed that the role of Cu^+ with d^{10} configuration is just to balance the charge (Cu acts just as a charge donor here) and does not have any important contribution for the conduction and valence band states except for donating one electron to the Pb-I framework as is reported for $CH_3NH_3^+$ and Cs^+ ions in $CH_3NH_3PbI_3$ and $CsPbI_3$, respectively.[22] However, our result is opposite to their conclusion that Cu is predictable to directly influence the electronic properties, e.g. Cu^+ has contributions to the band edges of the $CuPbX_3$ materials. Figure 3 shows the PDOS of the Pb 6s, Pb 6p, Cu 4s, Cu 3d and I 5p states. From the PDOS onto the Pb 6p and I 5p orbitals, it can be seen that the upper valence bands are predominantly contributed by Cu 4d and I 5p as well as the band above Fermi level is dominated by Cu 4s and I 5p hybridization, while the lower conduction bands are predominantly contributed by Pb 6p orbitals. Those

orbital components of each band can be seen more clearly in PDOS shown in Figure 3a-c. Complex bands between −3 and −1.5 eV are composed of I 5p and Cu 3d orbitals mixed slightly with Pb 6p and Cu 4s as hybridizing states. Furthermore, due to the hybridization of Cu 4s and X p orbitals the electron density at the Fermi energy is delocalized over the entire crystal. An important point is the existence of the bonding band of Cu 4s and I 5p above the Fermi energy should govern the transport and conductivity properties of the system. Importantly, through the sequence $CuPbCl_3$, $CuPbBr_3$, and $CuPbI_3$, the P and d levels approach one another, causing an increase in the P-d mixing. In our model, an increased mixing of P-d should decrease the width of the lower P band, a fact which is probably compensated by the increased spin-orbit interaction in going from $CuPbCl_3$ to $CuPbI_3$.

Because of the antibonding nature of Pb—I[26], the charge densities are localized at the VBM and CBM. Typically, when the band edges are composed of d orbitals, the absorption coefficient is large because the localized 3d orbital have a high DOS arising from their high degree of degeneracy. For the partial replacement of iodine by bromine and chlorine, the band structure of these materials changed into indirect bandgap as shown in Figure S3. This change of band structure from direct into indirect band structure may be due to the compression happening by the replacement of large iodine ion by small bromine and chlorine ions. Thus, the absorption coefficient for $CuPbI_3$ has been reported at 1.64 eV is $1.63xl0^5$ cm^{-1}, which is quite suitable for direct electronic transitions. The 3d level of Cu plays an important role in the electronic properties of $CuPbX_3$. The spatial extent of the d levels is large, and their energies are close to those of the P levels of the halogen. The P and d levels can, therefore, hybridize and thus significantly alter the chemical behavior of these compounds and hybridization of I 5p + Cu 4s lifting the valence band towards more positive and play a crucial role in tuning the energy band structure (band gap, band edge, and bandwidth, etc.) and, thus, in tailoring the optical properties.

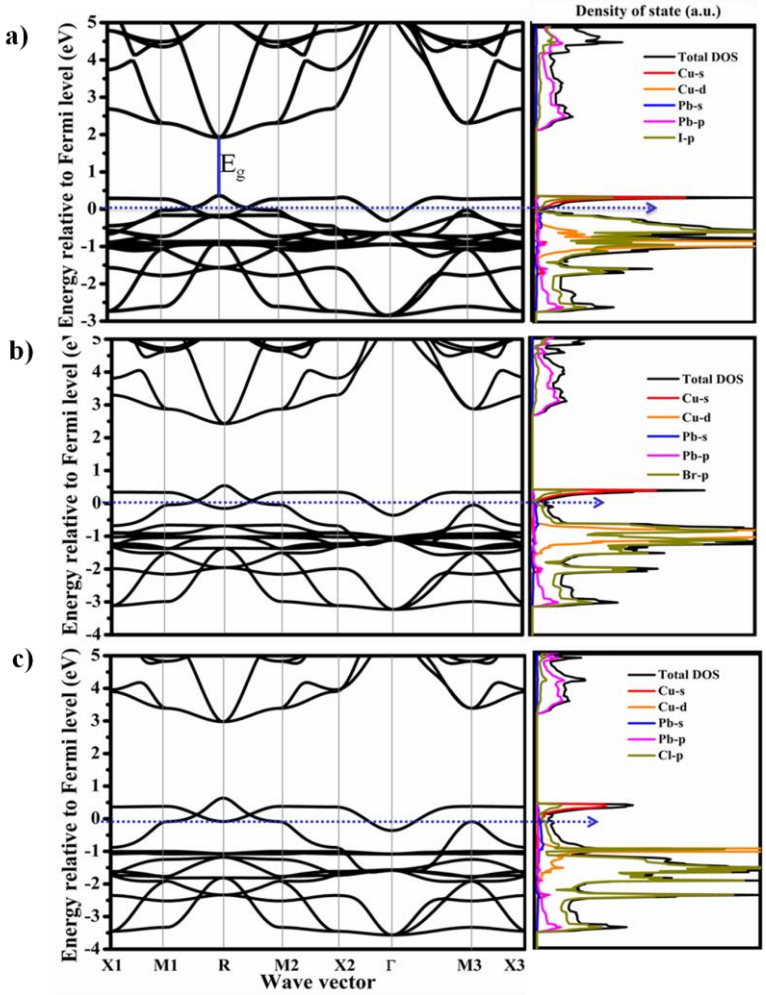

Figure 3 Band structure and PDOS of the pseudocubic a) $CuPbI_3$, b) $CuPbBr_3$ and c) $CuPbCl_3$ structures. The energy zero is at the VBM and the spin orbit coupling effect was not considered. Blue arrows are Fermi level at 0 eV. The participation of Cu 3d orbital in the valence band decrease from I to Cl.

Electronic and optical properties of $AgPbX_3$: The band structure and DOS for $AgPbI_3$ were calculated using similar computational approach and this material has shown direct band gap (1.57 eV i.e larger than the bandgap for $CuPbI_3$) indicating bandgap increase with size of A cation increase in ABX_3 structure. Its band structure and DOS are shown in Figure 4. Ag 4d orbital was not participating in $AgPbI_3$ valence band formation, while Cu 3d orbital was participating in $CuPbX_3$ valence band formation. The Ag 4d orbital was observed in the more negative energy and almost its interaction with I 5p was

negligible. However, Ag 4s was interacting with I-5p orbital above the Fermi level, tuning the band gap and reflects $AgPbI_3$ is p type semiconductor material due to the empty band Ag 4s hybridizing with I 5p above the Fermi level. For $AgPbI_3$, the CB is composed of the empty Pb 6p, whereas the VB is composed of the hybridized (I 5p, and above the Fermi level is (I 5p + Ag 4s orbitals) hybridization, with hybridization of I 5p + Ag 4s play a crucial role in tuning the energy band structure (band gap, band edge, and bandwidth, etc.) and, thus in tailoring the photophysical and optical properties.

Replacing iodide ion by bromide and chloride increased both the bandgap energy (1.57 eV to 2.33 eV) and the participation of d orbital in the valence band as shown in Figure 4a and 4b. This is opposite to the participation of Cu 3d orbital in $CuPbI_3$, which was observed decreasing its participation when iodide ion replaced by bromide and chloride.

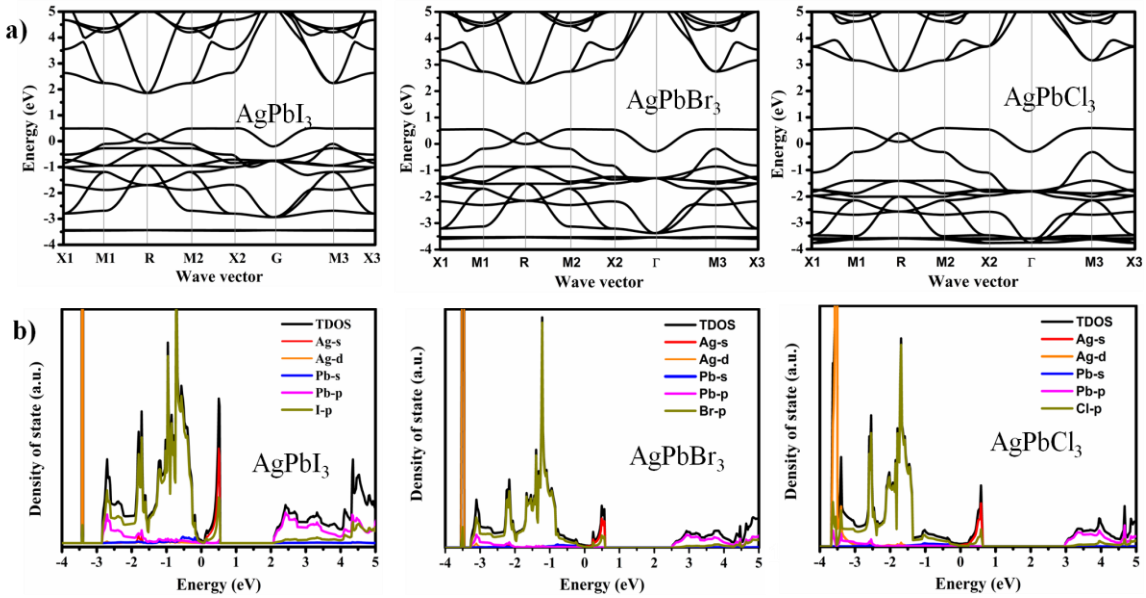

Figure 4 Computational study of $AgPbX_3$: a) Crystal structure, b) simulated X- ray diffraction c) band structure and PDOS of the pseudocubic $AgPbX_3$ structures. The energy zero is at the VBM. Band structure calculation was without considering spin orbit coupling effect.

Effect of A and X Size on bandgap and optical properties of $APbX_3$ (A =Cu, Ag, Cs and $CH_3NH_3^+$)

Figure 5 shows the effect of size on the optical bandgap of ternary lead halide perovskites. We observed that the band gap increase with increasing size of A ions and decreasing size of X ions. These chemical trends are important to understand and optimize this type of solar cell absorbers materials. We explain these trends by the above band structure analysis shown in Figure 3, Figure 4 and Figure S5: (i) Band gap dependence on the A ion and X ions. As Cu and Ag ions have contribution to the states near the Fermi surface, it affects the band gaps directly by modifying the valence band and indirectly by modifying the lattice constants of $CuPbX_3$ and $AgPbX_3$. But, Cs^+ and $CH_3NH_3^+$ cations affect the band gap only indirectly by modifying the lattice constants of $CsPbX_3$ and $CH_3NH_3PbX_3$.

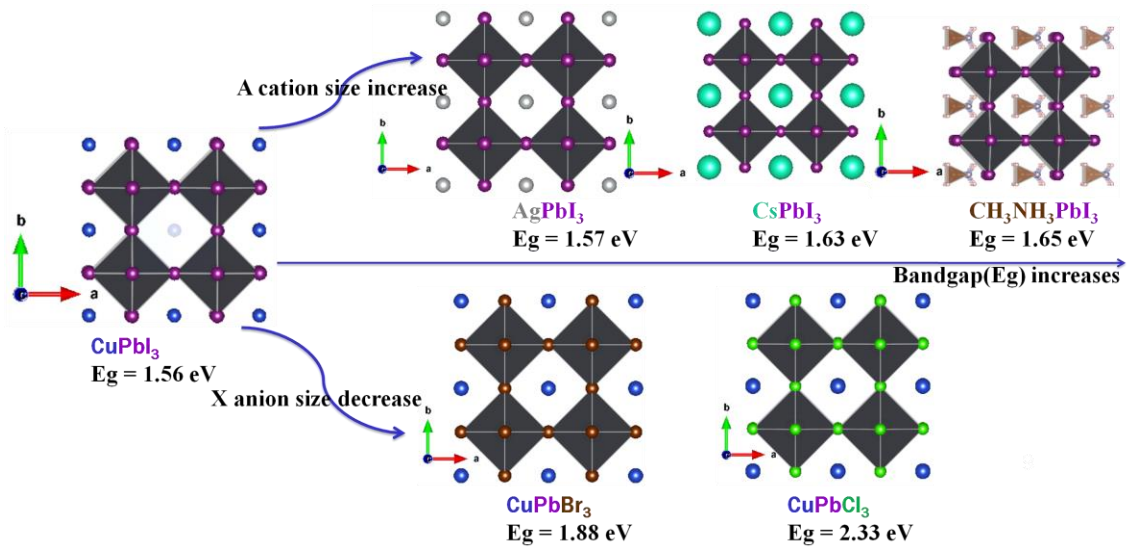

Figure 5 Effect of size of A cation and X anion on the bandgap of $APbX_3$ (A= Cu, Ag, Cs and $CH_3NH_3^+$ and X = I, Br, & Cl).

Since the size of Cu and Ag are almost similar and smaller than Cs and $CH_3NH_3^+$, the lattice constants of $CuPbX_3$ and $AgPbX_3$ are very close and smaller than $CsPbX_3$ and $CH_3NH_3PbX_3$. Then the smaller lattice constant caused by the smaller size of A can increase the strength of the Pb s–X p hybridization due to the smaller Pb–X bond. Because the VBM is an anti-bonding state of the hybridization, it is shifted down in energy when the coupling decreases, thus explaining the increased band gap with A varies from Cu to CH_3NH_3. (ii) Band gap dependence on the X ion. Since the VBM contains some X p characters and the energy levels of the p states of the X ions decrease from I to Cl, the VBM down-shifts and the band gap becomes larger from I to Cl. Based on these chemical trends, we can use band structure engineering methods to flexibly tune the electronic properties of this kind of materials, i.e., by forming alloys between them, it is possible to find or design new solar cell absorbers with better performances. Therefore, we can conclude that $CuPbX_3$ and $AgPbX_3$ are potential candidates as good solar cell materials similar to $CsPbX_3$ and $CH_3NH_3PbX_3$ perovskites.

As $CuPbI_3$, $CuPbBr_3$, $CuPbCl_3$, $AgPbI_3$, $AgPbBr_3$ and $AgPbCl_3$ are more promising new ternary perovskites materials for solar cells absorber and many other optoelectronic devices from the viewpoint of band gap as shown in figures 5 and 6, now we focus on these materials and compare their experimentally determined optical properties. Possibly the most excellent attribute of methylammonium cation based hybrid perovskites is that

their band gap can be tuned widely from the blue to the red spectral regions. Similarly, Cu+ and Ag+ cation based inorganic ternary perovskites have band gap tunable over wide range of blue to red spectral region. Such range is accomplished by replacing the halide. The valence and conduction bands of methylammonium cation based perovskites are determined by the PbI_6 inorganic octahedron. The organic cation does not contribute to these bands but modulates the band gap by modifying the lead-halide bond distance;[27-28] as a result, the shifts produced by substituting the organic cation are less pronounced than those produced by substitution of the halide.[27] The full tunability of the band gap for $CH_3NH_3PbX_3$ has been demonstrated for I–Br compositions[6, 29] and strongly suggested for Br– Cl compositions.[30-31] The valence and conduction bands of Cu^+ and Ag^+ based ternary perovskites are not only determined by the inorganic PbI_6 octahedron, but also by the Cu^+ and Ag^+. The role of Cu^+ and Ag^+ is not only to modulate the band gap but also by tuning the band structure. Therefore, we demonstrate the full tunability of $CuPbX_3$ and $AgPbI_3$ and we compared them with the results obtained from our calculation of $CsPbI_3$ and $CH_3NH_3PbI_3$ perovskites as shown in Figure 5. Changing the I–Cl ratio does not yield a change in band gap because of their much larger difference in ionic size.[32] Instead, phase segregation results.[33] However, changing in I-Br ($CuPbI_2Br$) and I-Cl ($CuPbI_2Cl$) ration change the direct band gap behavior of the cubic $CuPbI_3$ into indirect band gap behavior without phase segregation.

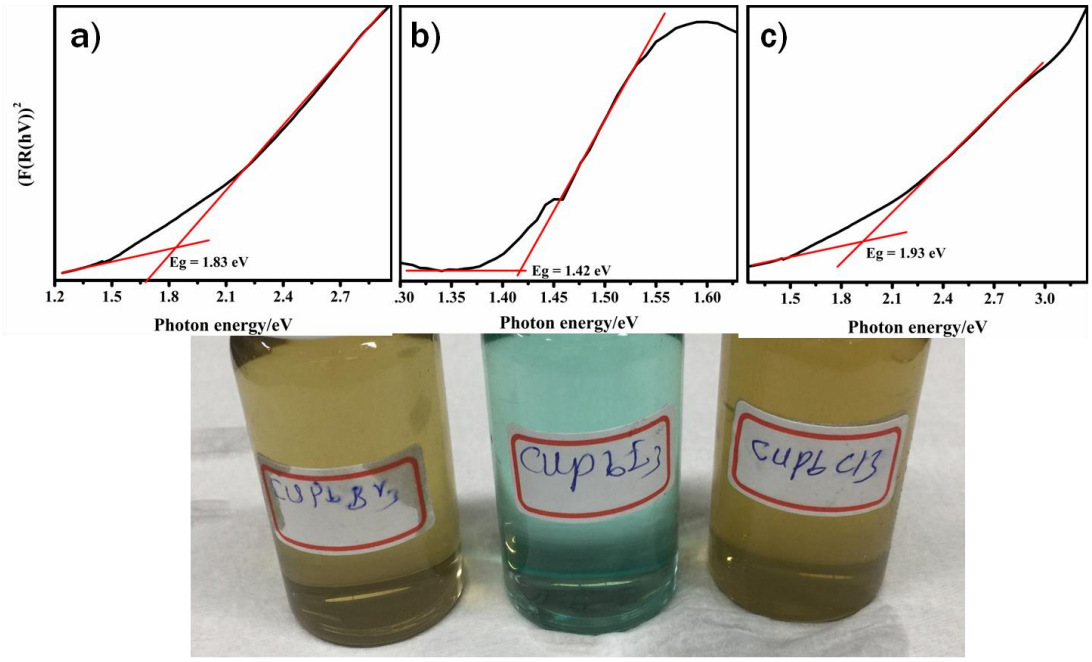

Figure 6 Experimentally determined band gap for a) $CuPbBr_3$, b) $CuPbI_3$ and c) $CuPbCl_3$

Summary

The materials community is currently witnessing a fundamental change in the way novel materials are designed and discovered for photovoltaic and other applications. A steady increase in computational power, accompanied by developments in quantum theory and algorithmic breakthroughs that allow for efficient yet accurate quantum mechanical computations, opens the door to computing properties of a wide range of materials that once seemed prohibitively expensive. We investigated Crystal structure, electronic and optical properties of $CuPbI_3$, $CuPbBr_3$ and $CuPbCl_3$ and $AgPbI_3$ material for fully inorganic perovskites solar cell application using computational methods. We found that these materials are suitable for solar cell purpose since their optical bandgap ranged from 1.54 – 2.33 eV by computational calculation and 1.42-1.80 eV by experimentally determined, which is similar to the $CH_3NH_3PbI_3$ hybrid perovskites. Furthermore, the VBM consists of the Cu 3d and halogen p orbital, whereas CBM is dominated by Pb 6p. Cu^+ has not only similar role for charge balance like the $CH_3NH_3^+$ cation, but also participating in valence bad formation, verifying that it has great contribution to the optical and electronic properties. However, Ag^+ participation in VB is less compared to Cu^+ due to the weak interaction of Ag 4d and halogen p orbitals observed. Their similarity is both Ag 4s and Cu 4s hybridized with halogen p orbitals above the Fermi level, tuning the band structure. Due to its direct bandgap and possibility of direct transition in this material, it is also expected to be suitable material for laser and light emitting device applications. This fully inorganic ternary metal (I) lead halide perovskites may be promising candidates for addressing the challenging issues regarding methylammonium lead halide perovskites such as instability in the presence of moisture and ambient atmosphere in general.

Acknowledgements

The financial support from the Ministry of Science and Technology (MoST) (104-3113-E-011-001-, 104-ET-E-001-ET, 103-2221-E-011-156-MY3, 102-2221-E-011-157), the Top University Projects(100H45140) and the Global Networking Talent 3.0 plan (NTUST 104DI005)) from the Ministry of Education of Taiwan, as well as the facilities

of support from National Taiwan University of Science and Technology (NTUST) and National Synchrotron Radiation Research Center (NSRRC), Hsinchu, Taiwan are acknowledged. We also thank the National center for High-performance Computing (NCHC) in Taiwan for providing computer resource and research facilities.

Conflict of interest: The authors declare no conflict of interest.

Referene

Energy & Environmental Sci

1. Bush, K. A.; Palmstrom, A. F.; Yu, Z. J.; Boccard, M.; Cheacharoen, R.; Mailoa, J. P.; McMeekin, D. P.; Hoye, R. L. Z.; Bailie, C. D.; Leijtens, T.; Peters, I. M.; Minichetti, M. C.; Rolston, N.; Prasanna, R.; Sofia, S.; Harwood, D.; Ma, W.; Moghadam, F.; Snaith, H. J.; Buonassisi, T.; Holman, Z. C.; Bent, S. F.; McGehee, M. D., 23.6%-efficient monolithic perovskite/silicon tandem solar cells with improved stability. *Nature Energy* **2017,** *2*, 17009.
2. Al-Ashouri, A.; Köhnen, E.; Li, B.; Magomedov, A.; Hempel, H.; Caprioglio, P.; Márquez, J. A.; Morales Vilches, A. B.; Kasparavicius, E.; Smith, J. A.; Phung, N.; Menzel, D.; Grischek, M.; Kegelmann, L.; Skroblin, D.; Gollwitzer, C.; Malinauskas, T.; Jošt, M.; Matič, G.; Rech, B.; Schlatmann, R.; Topič, M.; Korte, L.; Abate, A.; Stannowski, B.; Neher, D.; Stolterfoht, M.; Unold, T.; Getautis, V.; Albrecht, S., Monolithic perovskite/silicon tandem solar cell with >29% efficiency by enhanced hole extraction. *Science* **2020,** *370* (6522), 1300-1309.
3. Yin, W.-J.; Shi, T.; Yan, Y., Unique Properties of Halide Perovskites as Possible Origins of the Superior Solar Cell Performance. *Adv. Mater. (Weinheim, Ger.)* **2014,** *26* (27), 4653-4658.
4. Agiorgousis, M. L.; Sun, Y.-Y.; Zeng, H.; Zhang, S., Strong Covalency-Induced Recombination Centers in Perovskite Solar Cell Material CH3NH3PbI3. *J. Am. Chem. Soc.* **2014,** *136* (41), 14570-14575.
5. Wang, Q.; Shao, Y.; Xie, H.; Lyu, L.; Liu, X.; Gao, Y.; Huang, J., Qualifying composition dependent p and n self-doping in CH3NH3PbI3. *Appl. Phys. Lett.* **2014,** *105* (16), 163508.
6. Noh, J. H.; Im, S. H.; Heo, J. H.; Mandal, T. N.; Seok, S. I., Chemical Management for Colorful, Efficient, and Stable Inorganic–Organic Hybrid Nanostructured Solar Cells. *Nano Lett.* **2013,** *13* (4), 1764-1769.
7. Berhe, T. A.; Su, W.-N.; Chen, C.-H.; Pan, C.-J.; Cheng, J.-H.; Chen, H.-M.; Tsai, M.-C.; Chen, L.-Y.; Dubale, A. A.; Hwang, B.-J., Organometal halide perovskite solar cells: degradation and stability. *Energy & Environmental Science* **2016,** *9* (2), 323-356.
8. Berhe, T. A.; Cheng, J.-H.; Su, W.-N.; Pan, C.-J.; Tsai, M.-C.; Chen, H.-M.; Yang, Z.; Tan, H.; Chen, C.-H.; Yeh, M.-H.; Tamirat, A. G.; Huang, S.-F.; Chen, L.-Y.; Lee, J.-F.; Liao, Y.-F.; Sargent, E. H.; Dai, H.; Hwang, B.-J., Identification of the physical origin behind disorder, heterogeneity, and reconstruction and their correlation with the photoluminescence lifetime in hybrid perovskite thin films. *Journal of Materials Chemistry A* **2017,** *5* (39), 21002-21015.

9. Yang, W. S.; Noh, J. H.; Jeon, N. J.; Kim, Y. C.; Ryu, S.; Seo, J.; Seok, S. I., High-performance photovoltaic perovskite layers fabricated through intramolecular exchange. *Science* **2015,** *348* (6240), 1234-1237.
10. Saliba, M.; Matsui, T.; Seo, J.-Y.; Domanski, K.; Correa-Baena, J.-P.; Nazeeruddin, M. K.; Zakeeruddin, S. M.; Tress, W.; Abate, A.; Hagfeldt, A.; Gratzel, M., Cesium-containing triple cation perovskite solar cells: improved stability, reproducibility and high efficiency. *Energy Environ Sci* **2016,** *9* (6), 1989-1997.
11. Lee, J.-W.; Kim, D.-H.; Kim, H.-S.; Seo, S.-W.; Cho, S. M.; Park, N.-G., Formamidinium and Cesium Hybridization for Photo- and Moisture-Stable Perovskite Solar Cell. *Adv. Energy Mater.* **2015,** *5* (20), 1501310-n/a.
12. Service, R. F., Perovskite solar cells gear up to go commercial. *Science* **2016,** *354* (6317), 1214-1215.
13. Palmstrom, A. F.; Santra, P. K.; Bent, S. F., Atomic layer deposition in nanostructured photovoltaics: tuning optical, electronic and surface properties. *Nanoscale* **2015,** *7* (29), 12266-12283.
14. Pilania, G.; Balachandran, P. V.; Kim, C.; Lookman, T., Finding New Perovskite Halides via Machine Learning. *Frontiers in Materials* **2016,** *3* (19).
15. Li, C.; Lu, X.; Ding, W.; Feng, L.; Gao, Y.; Guo, Z., Formability of ABX3 (X = F, Cl, Br, I) halide perovskites. *Acta Crystallographica Section B* **2008,** *64* (6), 702-707.
16. Berhe, T. A.; Su, W. N.; Cheng, J. H.; Lin, M. H.; Ibrahim, K. B.; Kahsay, A. W.; Lin Li, C.; Tripathi, A. M.; Tang, M. T.; Hwang, B. J., Scalable Synthesis of Micron Size Crystals of CH3NH3PbI3 at Room Temperature in Acetonitrile via Rapid Reactive Crystallization. *ChemistrySelect* **2020,** *5* (11), 3266-3271.
17. Lang, L.; Yang, J.-H.; Liu, H.-R.; Xiang, H. J.; Gong, X. G., First-principles study on the electronic and optical properties of cubic ABX3 halide perovskites. *Phys. Lett. A* **2014,** *378* (3), 290-293.
18. Berhe, T. A. In *Room Temperature Synthesis, Mechanism and Stability Analysis of CH3NH3PbI3 and the Development of Transition metal (I) cation based New Inorganic Perovskites*, 2017.
19. Goldschmidt, V. M., *Skrifter Norske Videnskaps-Akad. Oslo. I Mathemat. Naturwiss. Klasse No 8* **1926**.
20. Naeem, R.; Yahya, R.; Mansoor, M. A.; Teridi, M. A. M.; Sookhakian, M.; Mumtaz, A.; Mazhar, M., Photoelectrochemical water splitting over mesoporous CuPbI3 films prepared by electrophoretic technique. *Monatshefte für Chemie - Chemical Monthly* **2017**, 1-9.
21. Kuku TA, A. S., Preparation, electrical and optical properties of evaporated thin films of CuPbI3. *International atomic energy agency, Triest, Italy* **1995**.
22. Zhao, Y.; Zhu, K., Organic-inorganic hybrid lead halide perovskites for optoelectronic and electronic applications. *Chem. Soc. Rev.* **2016,** *45* (3), 655-689.
23. Kieslich, G.; Goodwin, A. L., The same and not the same: molecular perovskites and their solid-state analogues. *Materials Horizons* **2017**.
24. Yin WJ, S. T., Yan Y Unusual defect physics in CH3NH3PbI3 perovskite solar cell absorber. *Appl. Phys. Lett.* **2014,** *104*, 063903.
25. Brivio F, W. A., Walsh A Structural and Electronic Properties of Hybrid Perovskites for High-Efficiency Thin-Film Photovoltaics from First-Principles. *Appl Mater* **2013,** *1*, 042111.

26. Umebayashi, T.; Asai, K.; Kondo, T.; Nakao, A., Electronic structures of lead iodide based low-dimensional crystals. *Physical Review B* **2003,** *67* (15), 155405.
27. Eperon, G. E.; Stranks, S. D.; Menelaou, C.; Johnston, M. B.; Herz, L. M.; Snaith, H. J., Formamidinium lead trihalide: a broadly tunable perovskite for efficient planar heterojunction solar cells. *Energy Environ Sci* **2014,** *7* (3), 982-988.
28. Mitzi, D. B., Solution-processed inorganic semiconductors. *J. Mater. Chem.* **2004,** *14* (15), 2355-2365.
29. Sadhanala, A.; Deschler, F.; Thomas, T. H.; Dutton, S. E.; Goedel, K. C.; Hanusch, F. C.; Lai, M. L.; Steiner, U.; Bein, T.; Docampo, P.; Cahen, D.; Friend, R. H., Preparation of Single-Phase Films of CH3NH3Pb(I1–xBrx)3 with Sharp Optical Band Edges. *J. Phys. Chem. Lett.* **2014,** *5* (15), 2501-2505.
30. G. Xing, N. M., S.S. Lim, N. Yantara, X. Liu, D. Sabba, M. Grätzel, S. Mhaisalkar, and T.C. Sum: , Low-temperature solution-processed wavelength-tunable perovskites for lasing. . *Nat. Mater.* **2014**, 476.
31. Kitazawa, N.; Watanabe, Y.; Nakamura, Y., Optical properties of CH3NH3PbX3 (X = halogen) and their mixed-halide crystals. *J. Mater. Sci.* **2002,** *37* (17), 3585-3587.
32. Colella, S.; Mosconi, E.; Fedeli, P.; Listorti, A.; Gazza, F.; Orlandi, F.; Ferro, P.; Besagni, T.; Rizzo, A.; Calestani, G.; Gigli, G.; De Angelis, F.; Mosca, R., MAPbI3-xClx Mixed Halide Perovskite for Hybrid Solar Cells: The Role of Chloride as Dopant on the Transport and Structural Properties. *Chemistry of Materials* **2013,** *25* (22), 4613-4618.
33. Pistor, P.; Borchert, J.; Fränzel, W.; Csuk, R.; Scheer, R., Monitoring the Phase Formation of Coevaporated Lead Halide Perovskite Thin Films by in Situ X-ray Diffraction. *J. Phys. Chem. Lett.* **2014,** *5* (19), 3308-3312.